ACS MATERIALS LETTERS

www.acsmaterialsletters.org

LETTER

Fabrication of Twin-Free Ultrathin NH_2-MIL-125(Ti) Membrane with *c*-Preferred Orientation Using Transition-Metal Trichalcogenides as Titanium Source

Yanwei Sun,[#] Yan Dong,[#] Yuyang Wu, Feng-Yen Shih, Chenhan Zhang, Huixia Luo,[*] Shi-Hsin Lin, and Yi Liu[*]

Cite This: *ACS Materials Lett.* 2022, 4, 55−60

Read Online

ACCESS | Metrics & More | Article Recommendations | Supporting Information

ABSTRACT: **In this study, layered TiS_3, a kind of transition-metal trichalcogenide, was applied as the titanium source of NH_2-MIL-125 during single-mode microwave-assisted secondary growth. Because of the appropriate Ti−S bond intensity and stability of TiS_3, the solvothermal reaction could be conducted under milder reaction conditions, resulting in the formation of a twin-free, highly *c*-oriented ultrathin NH_2-MIL-125(Ti) membrane. This membrane exhibited exceptional H_2 permeance while maintaining high H_2 permselectivity.**

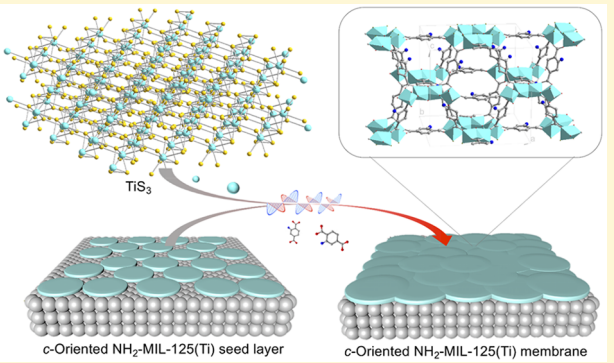

Metal−organic frameworks (MOF) exhibit tremendous potential for membrane-based separation, owing to the designable structures and tunable properties.[1] Nevertheless, membrane materials are generally constrained by the trade-off between permselectivity and permeability.[2] Microstructure manipulation has therefore become indispensable for polycrystalline MOF membranes to conquer the upper bound limit.[3] Among all the microstructural factors, it has been proven that the preferred orientation had a profound impact on gas permeation behavior through regulating the diffusion pathway and grain boundary defect density.[4] For instance, we found that maintaining the preferred *c*-orientation was beneficial for improving the H_2 permselectivity of the well-intergrown NH_2-MIL-125(Ti) membrane, owing to drastically decreased intercrystalline defects,[5] while simultaneous control of three-dimensional orientations of the NH_2-UiO-66 membrane resulted in concurrent enhancement of H_2/CO_2 permselectivity and H_2 permeability in comparison with their randomly or merely out-of-plane orientated counterparts.[6]

Oriented secondary growth has been considered as a practical approach for preparing highly oriented MOF membranes involving the oriented seed layer deposition and then in-plane secondary growth.[7] In terms of orientation control, effective suppression of undesired twin generation with no compromise in in-plane intergrowth has proven to be of vital importance in the process of secondary growth.

As mentioned above, a high-performance NH_2-MIL-125(Ti) membrane was successfully fabricated in our recent study. After depositing a closely packed seed monolayer with the facile ALIAS method, solvothermal epitaxial growth was employed to elimanate the open space remaining in the seed layer. It was found that using layered TiS_2 was indispensable for effective twin suppression, therefore fabricating the relevant membrane showing the desired microstructure. Because of weak van der Waals forces as well as relatively hight Ti−S bond strength, layered TiS_2 was susceptible to nucleophilic attack by NH_2−BDC ligands under harsh solvothermal conditions so that titanium species were released to the bulk solution slowly, which contributed to nucleation retardation in the bulk

Received: July 31, 2021
Accepted: November 24, 2021

https://doi.org/10.1021/acsmaterialslett.1c00452
ACS Materials Lett. 2022, 4, 55−60

solution and, therefore, effective twin suppression on the membrane surface.

Besides preferred orientation control, thickness reduction represents another reliable approach for decreasing the diffusion barrier and, therefore, increasing gas permeance of MOF membranes.[8] Conducting the reaction under mild conditions in a short period of time has proven to be effective for concurrently reducing membrane thickness and improving the preferred orientation of MOF membranes. Nevertheless, carrying out secondary growth under the aforementioned conditions commonly led to insufficient in-plane intergrowth between neighboring seeds and, therefore, high grain boundary defect density. With NH_2-MIL-125(Ti), a promising candidate for membrane-based CO_2 separation, as an example, our recent study indicated that in comparison with the conventional solvothermal approach, employing single-mode microwave-assisted heating enabled the significant reduction of reaction time so that undesired twin growth was effectively suppressed. As a result, a 500-nm-thick NH_2-MIL-125(Ti) membrane exhibiting *c*-preferred orientation was successfully fabricated. Nevertheless, maintaining a high reaction temperature remained necessary for ensuring membrane continuity. Mild fabrication of a thinner NH_2-MIL-125(Ti) membrane showing a higher degree of *c*-preferred orientation with no compromise in continuity is thus highly desired.

Herein, we sought to prepare NH_2-MIL-125(Ti) membranes with superior microstructure under milder reaction conditions in short reaction duration by an innovative titanium source. Transition-metal trichalcogenides (TMTCs) with the formula TX_3 (T represents transition metals and X represents chalcogens) have shown great potential in field-effect transistors and photodetectors based on their unusual ground states and collective-mode electronic transport.[9] Their potential as a metal source, however, has not been explored yet. Compared with their structural analogs, i.e., TMDCs, the M−X bond strength concerning the chemical stability should be different in view of their structural discrepancy. Herein, we compared their structural discrepancy by taking examples of TMDC TiS_2 and TMTC TiS_3. As shown in Figure 1, TiS_3 crystallizes in space group $P2_1/m$ of the monoclinic system and per unit cell is composed of two twisted prisms, parallel chains of triangular prisms bonded along the crystallographic *a*-axis forming sheets held together by van der Waals forces.[10] Different from TiS_2, there are two different kinds of S atoms within the TiS_3 framework, the sulfur atom serving as a bridge connected by two bridge titanium atoms and the remaining sulfur−sulfur pair bonded to a single titanium atom, forming four kinds of Ti−S bonds with lengths of 2.46, 2.49, 2.49, and 2.63 Å, respectively, all of which are longer than the Ti−S bond (2.43 Å) in TiS_2.[11] The formation energies of TiS_2 and TiS_3 were further calculated based on density functional theory (DFT),[12] and detailed computational results can be found in Table S1. Relevant caculation results indicated that TiS_2 had higher stability compared with TiS_3, since the formation energy of TiS_3 (0.978 eV) was much lower than that of TiS_2 (1.272 eV). We therefore deduced that, compared with TiS_2, TiS_3 should be more prone to nucleophilic attack by NH_2−BDC ligands under solvothermal conditions so that titanium species could be released to precursor solution under milder reaction conditions, thereby warranting the growth of thinner membrane as shown in Figure 1d.

Initially, we verified the feasibility for converting TiS_3 into NH_2-MIL-125(Ti) via solvothermal treatment. Layered TiS_3,

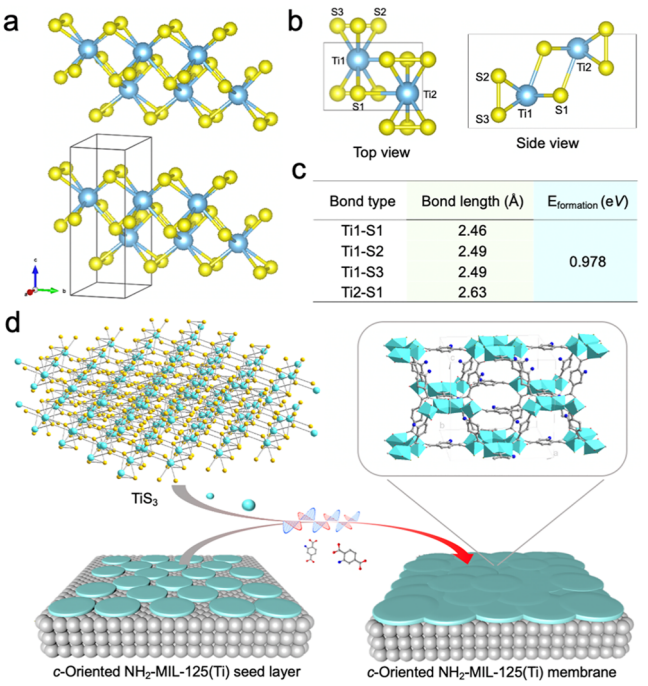

Figure 1. (a) Layered TiS_3 structure illustration. (b) Single unit cell of layered TiS_3 (structure models are produced using VESTA). (c) Structural parameters of TiS_3. (d) Schematic illustration of the formation of the twin-free ultrathin NH_2-MIL-125(Ti) membranes exhibiting *c*-preferred orientation using TiS_3 as the titanium precursor.

which was prepared via a conventional solid-state reaction method with Ti and S elements in the molar ratio of 1:3.2 sealed in evacuated quartz tubes, exhibited the typical ribbon-like morphology without any detected impurities (Figure S1). As shown in Figure 2a, solvothermal treatment at 160 °C for 96 h led to complete consumption of the TiS_3 source and the formation of aggregated truncated bipyramid-shaped NH_2-

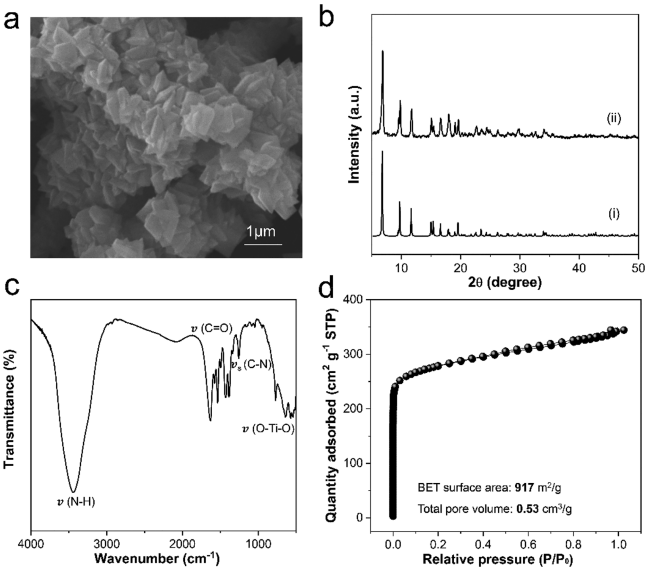

Figure 2. (a) Morphology of NH_2-MIL-125(Ti) powders derived from TiS_3. (b) XRD patterns of (i) simulated and (ii) prepared NH_2-MIL-125(Ti) powders, respectively. (c) FT-IR spectrum and (d) textural properties of prepared NH_2-MIL-125(Ti) powders.

https://doi.org/10.1021/acsmaterialslett.1c00452
ACS Materials Lett. 2022, 4, 55−60

MIL-125(Ti) powders with high crystallinity as evidenced by relevant XRD pattern (Figure 2b). FT-IR spectra of the prepared sample (Figure 2c) showed characteristic NH_2-MIL-125(Ti) vibration peaks.[13] To be specific, the peak at 1248 cm^{-1} was ascribed to the C−N stretching vibration from the aromatic amine, the vibration bands located between 800−1200 cm^{-1} could be attributed to benzene ring characteristic vibration, and the O−Ti−O vibration fell between 400 and 800 cm^{-1}. We studied the textural properties of TiS_3-derived NH_2-MIL-125(Ti) with nitrogen adsorption−desorption measurements. A typical type I adsorption isotherm was observed with decent surface areas (917 m^2/g) and total pore volumes (0.53 cm^3/g), which was similar to NH_2-MIL-125(Ti) synthesized with other titanium sources (Figure 2d).[14] The above results demonstrated that layered TiS_3 was a promising titanium source of NH_2-MIL-125 (Ti) without any compromise in crystallinity and porosity. It should be noted that owing to a decent Ti−S bonding strength, TiS_3 could be completely converted to NH_2-MIL-125(Ti) at lower reaction temperature (130 °C, shown in Figure S2); in contrast, the minimum temperature required for complete conversion of TiS_2 source reached 150 °C.[10]

The NH_2-MIL-125(Ti) membrane with desired microstructure was prepared as follows: Initially, the seed monolayer was obtained by self-assembling uniform NH_2-MIL-125(Ti) crystals with a disk-like shape (Figure S3).[15] As shown in Figure 3a, a ∼200-nm-thick seed layer was evenly deposited on

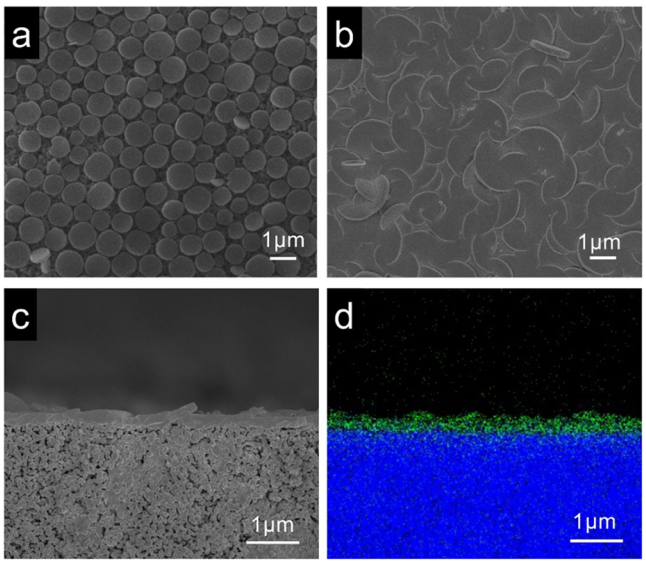

Figure 3. Morphology of (a) prepared NH_2-MIL-125(Ti) seed monolayer. (b) Top and (c) cross-section views of prepared NH_2-MIL-125(Ti) membranes obtained by conducting the reaction at 130 °C under single mode microwave heating. (d) EDXS mapping of Ti (color code: green) and Al (color code: blue) distributions at the cross-section of the NH_2-MIL-125(Ti) membrane.

the substrate surface (Figures 3a, S4). The XRD pattern showed that diffraction peaks assigned to (002), (004), and (008) planes were clearly visible (Figure 4b), confirming that the seed layer was dominantly *c*-oriented.

Subsequently, secondary growth was carried out on the *c*-oriented NH_2-MIL-125(Ti) seed layer. Nevertheless, it remained very challenging to suppress the undesired twin growth while simultaneously maintaining in-plane epitaxial

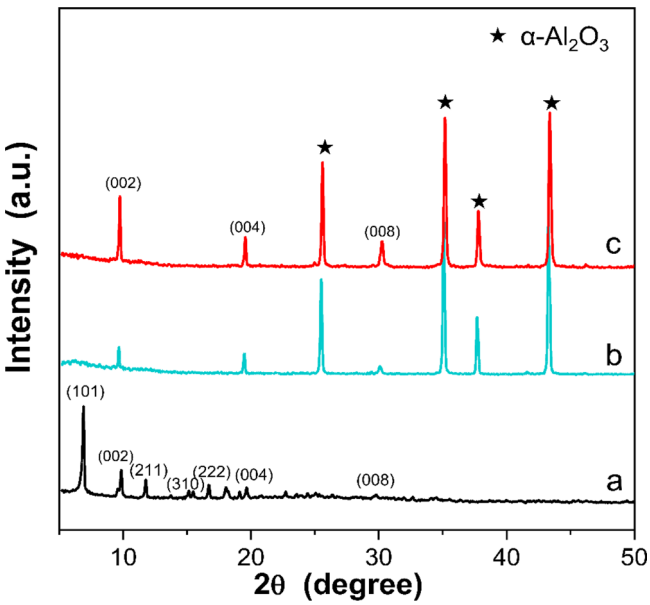

Figure 4. XRD patterns of relevant NH_2-MIL-125(Ti) (a) powders, (b) seed layers, and (c) membranes.

growth under conventional convective heating even under optimized synthetic conditions, owing to the high bulk nucleation rate of NH_2-MIL-125(Ti) and inferior rate of growth along the in-plane direction. Our recent study indicated that through combining single-mode microwave-assisted heating with a TiS_2 source, we could prepare a well-intergrown and preferentially *c*-oriented 500-nm-thick NH_2-MIL-125(Ti) membrane. Instead of TiS_2, herein TiS_3 served as the titanium source. Our experimental results indicated that the NH_2-MIL-125(Ti) membrane with superior microstructure could be readily prepared under milder reaction conditions (at 130 °C within 10 min) by using single-mode microwave-assisted heating. As shown in Figure 3b, a twin-free NH_2-MIL-125(Ti) membrane was obtained after secondary growth. Figure 3c confirmed that the membrane thickness was only 380 nm (Figure 3c), which was by far the thinnest membrane of the same type. Moreover, we found that the seed layer thickness exerted a profound effect on the membrane thickness. For instance, by using a ∼0.5-μm-thick seed layer, the thickness of the obtained NH_2-MIL-125(Ti) membrane increased to ∼800 nm (Figure S5). In addition, a clear interface between the NH_2-MIL-125(Ti) layer and the porous substrate was observed on the cross-sectional EDX mapping image (Figure 3d), indicating that the NH_2-MIL-125(Ti) membrane was only located on the substrate surface. Corresponding XRD data (Figure 4) showed (002), (004), and (008) characteristic peaks, which unambiguously confirmed that the membrane above remained dominantly oriented.

The lower reaction temperature required to form the NH_2-MIL-125(Ti) membrane with desired microstructure using TiS_3 as the titanium source could be ascribed to the weaker Ti−S bond strength, which enabled homogeneous release of a sufficient amount of titanium species under milder conditions. In contrast, with TiS_2 as the titanium source, the solvothermal reaction had to be conducted at temperatures no lower than 150 °C in order to release an equivalent amount of titanium species to sustain the desired growth rate of the seed layer (Figure S6). Along with decreased temperature, the rate of bulk nucleation and growth of NH_2-MIL-125(Ti) was

https://doi.org/10.1021/acsmaterialslett.1c00452
ACS Materials Lett. 2022, 4, 55−60

significantly decreased, resulting in a 5-fold decrease of twin density compared with that prepared with TiS_2 as the titanium source (Figure S7). In addition to twin suppression, the use of the TiS_3 source also significantly promoted the growth rate along the in-plane direction. According to the calculations, the relative in-plane epitaxial growth rate (v_i/v_o) of the seed layer using the TiS_3 source was approximately three times higher than that using the TiS_2 source (Table S2), thereby leading to a thinner NH_2-MIL-125(Ti) membrane without any compromise in continuity.

In addition, the influence of the secondary growth temperature on the final microstructure of the membrane using the TiS_3 source was further investigated. It was found that maintaining the reaction temperature at 130 °C was indispensable for the desired microstructure (Figure S8). Lowering the reaction temperature to 120 °C led to poor intergrowth between adjacent seeds, while increasing the reaction temperature to 150 °C inevitably increased membrane thickness. Simultaneously, the prepared membrane could not maintain a comparable degree of preferred *c*-orientation as evidenced by the corresponding XRD pattern (Figure S9). This could largely be attributed to excessive nucleation in the bulk solution at the higher temperature. Moreover, the solids that sedimented at the bottom of the vessels after the reaction at different temperatures were analyzed. As confirmed by XRD patterns (Figure S11), we found that characteristic peaks of TiS_3 still existed while no NH_2-MIL-125(Ti) phase appeared after solvothermal treatment under 130 °C, thereby implying effective prevention of the bulk nucleation. In contrast, in the case that the reaction temperature increased to 150 °C, not only was the crystalline structure of TiS_3 particles severely damaged, but substantial yellow particles, i.e., NH_2-MIL-125(Ti) powders, were formed in the reaction medium simultaneously (Figures S10, S11), which inevitably led to the generation of substantial twin crystals.

Finally, a gas permeation test was performed on a Wicke–Kallenbach setup (Figure S12). As shown in Figure 5, the H_2 permeance was much higher than that of other larger gas molecules, owing to the much higher diffusion coefficient of the former through the membrane. The ideal H_2/CO_2, H_2/N_2, and H_2/CH_4 selectivity attained 13.5, 10.1, and 10.9, respectively (Table S3). Figure S13 indicated that the separation performance of the membranes toward the H_2/CO_2 gas pair easily exceeded the Robeson 2008 upper-bound limits for polymer membranes. In particular, we noted that the H_2 permeance (840 GPU) was the highest in comparison with all other neat NH_2-MIL-125(Ti) membranes (Table S4),[5,16] demonstrating the significance of the concurrent preferred orientation and thickness control in their separation performance enhancement. Compared with other 6 Å pore-sized molecular sieve membranes, our membrane exhibited comparable H_2 permeance and H_2/CO_2 selectivity, although their overall H_2/CO_2 separation performances may be lower than those of some small pore-sized MOF membranes which were intrinsically more H_2/CO_2 selective (Table S5).

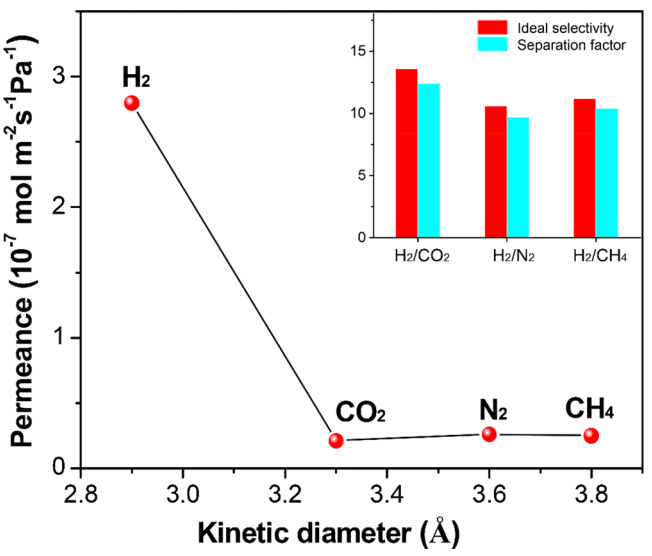

Figure 5. Permeance of single gases through prepared NH_2-MIL-125(Ti) membrane under ambient conditions (the inset shows detailed results of selectivity).

It was worth noting that a higher number of missing linkers per Ti-oxo cluster within the framework was caused by using the TiS_3 source, as confirmed by the TGA and N_2 adsorption/desorption results (Figures S14, S15). Accordingly, TiS_3-derived NH_2-MIL-125(Ti) exhibited higher CO_2 uptake (3.2 mmol g^{-1}, shown in Figure S16) in comparion with TiS_2-derived NH_2-MIL-125(Ti), which in turn promoted faster diffusion of CO_2 molecules through the membrane; simultaneously, TiS_3-derived NH_2-MIL-125(Ti) exhibited wider pore aperture distribution. Figure S15b indicated that the pore aperture of TiS_3-derived NH_2-MIL-125(Ti) was centered at ~5.8 Å and ~8 Å, respectively, which were both larger than that of the TiS_2-derived counterpart (~5.6 Å). Pore aperture expansion inevitably weakened the molecular sieving ability of the membrane. As a result, the prepared membrane exhibited decent permselectivity toward the H_2/CO_2 gas pair.

To summarize, with novel TMTCs (e.g., TiS_3) as a titanium source, herein we successfully prepared qualified NH_2-MIL-125(Ti) by treatment with a NH_2–BDC containing solution under solvothermal conditions. Moreover, through combining the TiS_3 source with single-mode microwave-assisted heating, a twin-free and ultrathin NH_2-MIL-125(Ti) membrane showing *c*-preferred orientation could be prepared under much milder reaction conditions, owing to the weaker Ti–S bond strength compared with that of TiS_2. It was noteworthy that employing TiS_3 as the titanium source effectively suppressed the generation of twins and promoted growth of the seed layer along the in-plane direction, thereby leading to reduced membrane thickness. Prepared membranes displayed exceptional H_2 permeance and high permselectivity towatds the H_2/CO_2 gas pair. It is expected that TMTCs could serve as a competitive metal precusor for the controllable synthesis and microstructure manipulation of various MOF membranes.

■ ASSOCIATED CONTENT

Supporting Information

The Supporting Information is available free of charge at https://pubs.acs.org/doi/10.1021/acsmaterialslett.1c00452.

Experimental procedures, characterization data, and gas separation performance of NH_2-MIL-125(Ti) membranes (PDF)

■ AUTHOR INFORMATION

Corresponding Authors

Yi Liu – *State Key Laboratory of Fine Chemicals, School of Chemical Engineering, Dalian University of Technology,*

https://doi.org/10.1021/acsmaterialslett.1c00452
ACS Materials Lett. 2022, 4, 55–60

Ganjingzi District, Dalian 116024, China; orcid.org/0000-0002-2073-4832; Email: diligenliu@dlut.edu.cn

Huixia Luo − *School of Materials Science and Engineering, State Key Laboratory of Optoelectronic Materials and Technologies, Key Lab of Polymer Composite & Functional Materials, Guangzhou Key Laboratory of Flexible Electronic Materials and Wearable Devices, Sun Yat-Sen University, Guangzhou 510275, China;* orcid.org/0000-0003-2703-5660; Email: luohx7@mail.sysu.edu.cn

Authors

Yanwei Sun − *State Key Laboratory of Fine Chemicals, School of Chemical Engineering, Dalian University of Technology, Ganjingzi District, Dalian 116024, China*

Yan Dong − *School of Materials Science and Engineering, State Key Laboratory of Optoelectronic Materials and Technologies, Key Lab of Polymer Composite & Functional Materials, Guangzhou Key Laboratory of Flexible Electronic Materials and Wearable Devices, Sun Yat-Sen University, Guangzhou 510275, China; Key Laboratory of Functional Molecular Solids, Ministry of Education, College of Chemistry and Materials Science, Anhui Normal University, Wuhu 241002, China*

Yuyang Wu − *State Key Laboratory of Fine Chemicals, School of Chemical Engineering, Dalian University of Technology, Ganjingzi District, Dalian 116024, China*

Feng-Yen Shih − *Department of Materials and Optoelectronic Science, Center of Crystal Research, National Sun Yat-sen University, Kaohsiung 804, Taiwan*

Chenhan Zhang − *State Key Laboratory of Fine Chemicals, School of Chemical Engineering, Dalian University of Technology, Ganjingzi District, Dalian 116024, China*

Shi-Hsin Lin − *Department of Materials and Optoelectronic Science, Center of Crystal Research, National Sun Yat-sen University, Kaohsiung 804, Taiwan*

Complete contact information is available at: https://pubs.acs.org/10.1021/acsmaterialslett.1c00452

Author Contributions

#The manuscript was written through contributions of all authors. All authors have given approval to the final version of the manuscript. Yanwei Sun and Dong Yan contributed equally to this work.

Notes

The authors declare no competing financial interest.

■ ACKNOWLEDGMENTS

Yi Liu is grateful to National Natural Science Foundation of China (22078039, 21176231), Science and Technology Innovation Fund of Dalian (2020JJ26GX026), Fok Ying-Tong Education Foundation of China (171063), Science Fund for Creative Research Groups of the National Natural Science Foundation of China (22021005), Liaoning Revitalization Talents Program (XLYC1807084), and the Technology Innovation Team of Dalian University of Technology (DUT2017TB01) for the financial support. Huixia Luo is grateful to the National Natural Science Foundation of China (11922415), Guangdong Basic and Applied Basic Research Foundation (2019A1515011718), the Fundamental Research Funds for the Central Universities (19lgzd03), Key Research & Development Program of Guangdong Province, China (2019B110209003), and the Pearl River Scholarship Program of Guangdong Province Universities and Colleges (20191001).

■ REFERENCES

(1) (a) Bux, H.; Liang, F.; Li, Y.; Cravillon, J.; Wiebcke, M.; Caro, J. Zeolitic imidazolate framework membrane with molecular sieving properties by microwave-assisted solvothermal synthesis. *J. Am. Chem. Soc.* **2009**, *131*, 16000−16001. (b) Liu, Y.; Ng, Z.; Khan, E. A.; Jeong, H. K.; Ching, C.; Lai, Z. Synthesis of continuous MOF-5 membranes on porous α-alumina substrates. *Microporous Mesoporous Mater.* **2009**, *118*, 296−301. (c) Liu, Y.; Hu, E.; Khan, E. A.; Lai, Z. Synthesis and characterization of ZIF-69 membranes and separation for CO_2/CO mixture. *J. Membr. Sci.* **2010**, *353*, 36−40.

(2) Park, H. B.; Kamcev, J.; Robeson, L. M.; Elimelech, M.; Freeman, B. D. Maximizing the right stuff: The trade-off between membrane permeability and selectivity. *Science* **2017**, *356*, eaab0530.

(3) (a) Liu, Y.; Ban, Y.; Yang, W. Microstructural engineering and architectural design of metal-organic framework membranes. *Adv. Mater.* **2017**, *29*, 1606949. (b) Zhang, C.; Wu, B. H.; Ma, M. Q.; Wang, Z.; Xu, Z. K. Ultrathin metal/covalent−organic framework membranes towards ultimate separation. *Chem. Soc. Rev.* **2019**, *48*, 3811−3841.

(4) (a) Mao, Y.; Su, B.; Cao, W.; Li, J.; Ying, Y.; Ying, W.; Hou, Y.; Sun, L.; Peng, X. Specific oriented metal−organic framework membranes and their facet-tuned separation performance. *ACS Appl. Mater. Interfaces* **2014**, *6*, 15676−15685. (b) Zhong, Z.; Yao, J.; Chen, R.; Low, Z.; He, M.; Liu, J. Z.; Wang, H. Oriented two-dimensional zeolitic imidazolate framework-L membranes and their gas permeation properties. *J. Mater. Chem. A* **2015**, *3*, 15715−15722. (c) Friebe, S.; Geppert, B.; Steinbach, F.; Caro, J. Metal−organic framework UiO-66 Layer: a highly oriented membrane with good selectivity and hydrogen permeance. *ACS Appl. Mater. Interfaces* **2017**, *9*, 12878−12885.

(5) Sun, Y.; Liu, Y.; Caro, J.; Guo, X.; Song, C.; Liu, Y. In-plane epitaxial growth of highly c-oriented NH_2-MIL-125(Ti) membranes with superior H_2/CO_2 selectivity. *Angew. Chem., Int. Ed.* **2018**, *57*, 16088−16093.

(6) Sun, Y.; Song, C.; Guo, X.; Liu, Y. Concurrent manipulation of out-of-plane and regional in-plane orientations of NH_2-UiO-66 membranes with significantly reduced anisotropic grain boundary and superior H_2/CO_2 separation performance. *ACS Appl. Mater. Interfaces* **2020**, *12*, 4494−4500.

(7) Ma, X.; Wan, Z.; Li, Y.; He, X.; Caro, J.; Huang, A. Anisotropic gas separation in oriented ZIF-95 membranes prepared by vapor-assisted in-plane epitaxial growth. *Angew. Chem., Int. Ed.* **2020**, *59*, 20858−20862.

(8) Wang, S.; Liu, J.; Pulido, B.; Li, Y.; Mahalingam, D.; Nunes, S. P. Oriented zeolitic imidazolate framework (ZIF) nanocrystal films for molecular separation membranes. *ACS Appl. Nano Mater.* **2020**, *3*, 3839−3846.

(9) (a) Li, M.; Dai, J.; Zeng, X. C. Tuning the electronic properties of transition-metal trichalcogenides via tensile strain. *Nanoscale* **2015**, *7*, 15385−15391. (b) Sivadas, N.; Daniels, M. W.; Swendsen, R. H.; Okamoto, S.; Xiao, D. Magnetic ground state of semiconducting transition metal trichalcogenide monolayers. *Phys. Rev. B: Condens. Matter Mater. Phys.* **2015**, *91*, 235425. (c) Gilbert, S. J.; Yi, H.; Chen, J. S.; Yost, A. J.; Dhingra, A.; Abourahma, J.; Lipatov, A.; Avila, J.; Komesu, T.; Sinitskii, A.; Asensio, M. C.; Dowben, P. A. Effect of band symmetry on photocurrent production in quasi-one-dimensional transition-Metal trichalcogenides. *ACS Appl. Mater. Interfaces* **2020**, *12*, 40525−40531.

(10) Sun, Y.; Hu, S.; Song, C.; Miao, S.; Jiang, Z.; Jiang, X.; Zhao, J.; Guo, X.; Liu, Y. Two-dimensional transition metal dichalcogenides as metal sources of metal−organic frameworks. *Chem. Commun.* **2018**, *54*, 3664−3667.

(11) (a) Furuseth, S.; Brattas, L.; Kjekshus, A. On the crystal structures of TiS_3, ZrS_3, $ZrSe_3$, $ZrTe_3$, HfS_3, and $HfSe_3$. *Acta Chem. Scand., Ser. A* **1975**, *29*, 623−631. (b) Jin, Y.; Li, X.; Yang, J. Single layer of MX_3 (M = Ti, Zr; X = S, Se, Te): a new platform for nano-

electronics and optics. *Phys. Chem. Chem. Phys.* **2015**, *17*, 18665−18669. (c) Island, J. O.; Biele, R.; Barawi, M.; Clamagirand, J. M.; Ares, J. R.; Sánchez, C.; van der Zant, H. S. J.; Ferrer, I. J.; D'Agosta, R.; Castellanos-Gomez, A. Titanium trisulfide (TiS_3): a 2D semiconductor with quasi-1D optical and electronic properties. *Sci. Rep.* **2016**, *6*, 22214.

(12) (a) Kresse, G.; Furthmüller, J. Efficient iterative schemes for ab initio total-energy calculations using a plane-wave basis set. *Phys. Rev. B: Condens. Matter Mater. Phys.* **1996**, *54*, 11169−11186. (b) Kresse, G.; Joubert, D. From ultrasoft pseudopotentials to the projector augmented-wave method. *Phys. Rev. B: Condens. Matter Mater. Phys.* **1999**, *59*, 1758−1775.

(13) (a) Fu, Y.; Sun, D.; Chen, Y.; Huang, R.; Ding, Z.; Fu, P. X.; Li, P. Z. An amine-functionalized titanium metal-organic framework photocatalyst with visible-light-induced activity for CO_2 reduction. *Angew. Chem., Int. Ed.* **2012**, *51*, 3364−3367. (b) Wu, Z.; Huang, X.; Zheng, H.; Wang, P.; Hai, G.; Dong, W.; Wang, G. Aromatic heterocycle-grafted NH_2-MIL-125(Ti) via conjugated linker with enhanced photocatalytic activity for selective oxidation of alcohols under visible light. *Appl. Catal., B* **2018**, *224*, 479−487.

(14) Sohail, M.; Yun, Y. N.; Lee, E.; Kim, S. K.; Cho, K.; Kim, J. N.; Kim, T. W.; Moon, J. H.; Kim, H. Synthesis of Highly Crystalline NH_2-MIL-125 (Ti) with s-shaped water isotherms for adsorption heat transformation. *Cryst. Growth Des.* **2017**, *17*, 1208−1213.

(15) Hu, S.; Liu, M.; Li, K.; Zuo, Y.; Zhang, A.; Song, C.; Zhang, G.; Guo, X. Solvothermal synthesis of NH_2-MIL-125(Ti) from circular plate to octahedron. *CrystEngComm* **2014**, *16*, 9645−9650.

(16) (a) Friebe, S.; Mundstock, A.; Unruh, D.; Renz, F.; Caro, J. NH_2-MIL-125 as membrane for carbon dioxide sequestration: thin supported MOF layers contra Mixed-Matrix-Membranes. *J. Membr. Sci.* **2016**, *516*, 185−193. (b) Sun, Y.; Song, C.; Guo, X.; Hong, S.; Choi, J.; Liu, Y. Microstructural optimization of NH_2-MIL-125 membranes with superior H_2/CO_2 separation performance by innovating metal sources and heating modes. *J. Membr. Sci.* **2020**, *616*, 118615.

https://doi.org/10.1021/acsmaterialslett.1c00452
ACS Materials Lett. 2022, 4, 55−60